Mechanism of Action of Cytotoxic Cyclotides: Cycloviolacin O2 Disrupts Lipid Membranes

Erika Svangård,[†] Robert Burman,[†] Sunithi Gunasekera,[†] Henrik Lövborg,[‡] Joachim Gullbo,[‡] and Ulf Göransson*[,†]

Division of Pharmacognosy, Department of Medicinal Chemistry, Biomedical Centre, Uppsala University, Uppsala, Sweden, and Division of Clinical Pharmacology, Department of Medical Sciences, University Hospital, Uppsala University, Uppsala, Sweden

Received January 5, 2007

In recent years, the cyclotides have emerged as the largest family of naturally cyclized proteins. Cyclotides display potent cytotoxic activity that varies with the structure of the proteins, and combined with their unique structure, they represent novel cytotoxic agents. However, their mechanism of action is yet unknown. In this work we show that disruption of cell membranes plays a crucial role in the cytotoxic effect of the cyclotide cycloviolacin O2 (**1**), which has been isolated from *Viola odorata*. Cell viability and morphology studies on the human lymphoma cell line U-937 GTB showed that cells exposed to **1** displayed disintegrated cell membranes within 5 min. Functional studies on calcein-loaded HeLa cells and on liposomes showed rapid concentration-dependent release of their respective internal contents. The present results show that cyclotides have specific membrane-disrupting activity.

Cyclotides are plant proteins characterized by an extraordinary structure: their N- and C-termini are joined by an ordinary peptide bond to form a continuously circular amide backbone. In addition, six of their approximately 30 amino acid residues are cysteines that form three disulfide bonds arranged in a cystine knot motif, as shown in Figure 1. These structural features are strictly conserved within this protein family, and they define the so-called cyclic cystine knot (CCK) motif,[1−3] which gives the cyclotides increased thermal, enzymatic, and chemical stability compared to linear peptides.[4,5]

Today, more than 80 cyclotides have been isolated from the Violaceae and Rubiaceae plant families, and they form the largest known family of genetically encoded cyclic proteins.[6−10] They display a range of biological activities, including uterotonic,[11] hemolytic,[12,13] antimicrobial,[14] anti-HIV,[15] antifouling,[16] and insecticidal[17] activities. Together with their remarkable stability this makes the CCK motif of great interest as a scaffold in protein engineering for potential pharmaceutical and agricultural applications.[18,19]

Despite the number of reported biological activities and the great interest in the cyclotides, the mechanism of action has not yet been established for any of these effects. Even if not all of the effects have been shown for a single cyclotide, it is conceivable that there might be a common mechanism of action for at least some of the effects. In fact, it has been suggested that a mechanism involving membrane interactions may explain their antimicrobial and hemolytic activities based on their structural resemblance (with the exception of their circular backbone) to other antimicrobial peptides that have such a mechanism of action.[7,20−22]

In our previous work we have shown that cyclotides represent a novel class of cytotoxic agents that display strong activity in a dose-dependent manner.[23,24] The cytotoxic activity was maintained throughout a cell line panel consisting of 10 human tumor cell lines, including solid tumor cells, and toward primary cultures of tumor cells from patients. In addition, the activity profile for cyclotides tested in the panel, which is designed to represent defined types of drug resistance, differs significantly from those of antitumor drugs in clinical use. This suggests a new mode of action. Sparked by these results and the fact that the tested cyclotides also display a definite structure−activity relationship,[23,24] we recently reported a detailed study of the most potent of the tested cyclotides, cycloviolacin O2 (**1**), which has been isolated from *Viola odorata* L. (Violaceae).[25] In this study we showed that a glutamic acid residue, which is conserved in the cyclotide family, plays a crucial role for the cytotoxic activity and that at least one cationic residue is required to maintain activity at low cyclotide concentrations.

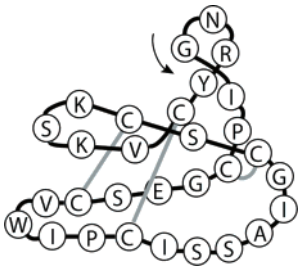

Figure 1. Sequence and schematic structure of cycloviolacin O2 (**1**). The solid black line represents the peptide backbone, and the sequence is shown by the one-letter codes for each amino acid. Note the unique features of the CCK motif: a cyclic backbone and three stabilizing disulfide bonds (in gray). These disulfides are arranged in a cystine knot; that is, two of the disulfides form a ring structure together with the backbone connecting the four cysteines, while the third disulfide is threaded through the ring. The arrow shows the direction of the genetic translation of the sequence.

In the present work we have used the same peptide, **1**, to characterize the mode of action of the cytotoxic effect of this cyclotide toward human cancer cells. First, we have characterized the kinetics of the effect using the same fluorescent microculture cytotoxicity assay (FMCA) as was used for the cell line panel,[23,24] and by microscopy studies. Second, we describe the morphology of treated cells. Then, we have assessed specifically the membrane effects of the cyclotide using cells loaded with calcein and a liposome-based assay.

Results and Discussion

To characterize the mechanism of action of **1**, we first established the kinetics of the cytotoxic effects using the FMCA and the U-937 GTB human lymphoma cell line. Cell survival was measured at 4, 8, 24, and 72 h. As shown in Figure 2, the concentration−response curves for the different time points essentially overlap, including the very steep shape of the curve between no and full effect. Following that overlap, the IC_{50} values did not show any significant difference at the different time points. Thus, the results showed that **1** achieves its full effect within 4 h, and the similar shape of

* Author to whom correspondence should be addressed. Tel: +46 18 471 50 31. Fax: +46 18 50 91 01. E-mail: ulf.goransson@fkog.uu.se.
[†] Biomedical Centre.
[‡] University Hospital.

10.1021/np070007v CCC: $37.00
Published on Web 03/23/2007

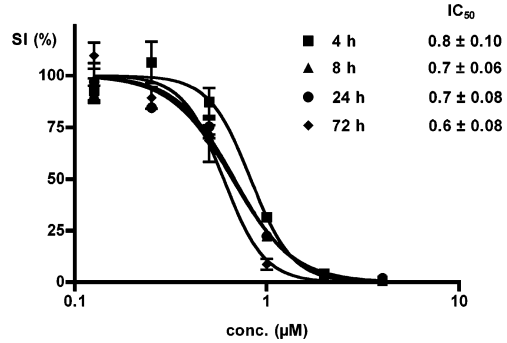

Figure 2. Kinetics in the FMCA. The human lymphoma cell line was exposed to cycloviolacin O2 (**1**) for 4, 8, 24, and 72 h, and cell viability was assessed using the FMCA. Each point represents the mean, while the error bars indicate ±SEM.

the curves indicates similar mechanisms of action throughout this time interval.

As 4 h is the shortest possible end-point in the FMCA, we then turned to microscopy studies for time points under 4 h. Microscopy slides of cells incubated with 4 μM (**1**) were then prepared at 5 min, 15 min, 30 min, 1 h, 2 h, 4 h, and 24 h. This concentration was chosen on the basis of the results in the FMCA, in which it was the lowest concentration to give a 100% effect. Living versus dead cells were then counted manually and compared to the control. Figures 3A and 3B exemplify the difference between the control and the cells exposed to **1**. The morphology of the cells exposed to the cyclotide was characterized by disrupted cell membranes. In comparison, we also exposed cells to markers for apoptosis and necrosis in separate experiments. As shown in Figures 3C and 3D, respectively, cells exposed to etoposide, which induces apoptosis, showed condensed and fragmented nuclei but intact membranes, while cells exposed to Triton X-100 displayed predominantly disintegrated cell membranes similar to the effect caused by **1**.

Cycloviolacin O2 (**1**) rapidly induced cell death, as shown by Figures 4A−D; cells with disrupted membranes were observed already after 5 min and more than 60% of the cells were dead after 1 h. Both gross morphology and the rapid onset indicated that necrosis rather than apoptosis is the mechanism of action. The percentages of cells classified as viable, necrotic, and apoptotic at the different time points are summarized in Figure 5. While these results point toward membrane disruption as the mechanism of action, the nature of the effect on the membrane is still unclear. Hence to specifically examine the effects on the lipid membrane, we then turned to functional assays that specifically measure membrane leakage, on both cells and liposomes.

For the calcein cell assay, HeLa cells were loaded with calcein acetoxymethyl ester (calcein-AM), which passes through the cell membrane and subsequently is hydrolyzed by the cell. The hydrolyzed calcein is thus entrapped in the cytoplasm.[26] Intact cells show an intense fluorescence, which decreases with induced calcein release/leakage. In our setup, the fluorescent signal of individual cells was measured with an automated fluorescence microscopic imaging system, which was set to monitor the area close to the cell nucleus. As shown in Figure 6 there was no leakage at 1 μM (**1**) over a time period of 4 h. At 5 μM, there was a time-dependent increase in calcein leakage, which was accelerated at the higher concentration. At that concentration (10 μM), the effect is very rapid: the fluorescence was decreased considerably compared to the control within 5 min. Notably, cell integrity is destroyed by **1** at similar concentrations and with similar kinetics to those seen in the microscopy studies, which indicates a similar mode of action.

Liposomes were then used to specifically examine the effects of **1** on lipid membranes. This assay was developed originally to identify transmembrane pore-forming peptides[27] and is based on the formation of a strongly fluorescent complex of terbium and dipicolinic acid (Tb^{3+}/DPA) in the presence of membrane-disrupting or pore-forming agents. Cycloviolacin O2 (**1**) showed a concentration-dependent effect on POPC liposomes in this assay, as shown in Figure 7. The EC_{50} value of **1** was 14.3 μM, which corresponds to a peptide-to-lipid molar ratio (P/L) of 6.5. As in previous assays, the onset was rapid; a time study showed that **1** achieved full effect within minutes (data not shown). However, for practical reasons, a 1 h incubation was used as the standard in this particular assay. For the reference peptide alamethicin,[28] the concentration−response curve was shifted to the left and the EC_{50} value was calculated to be 0.4 μM; that is, P/L = 0.2. In addition, the slope of the curve changed and the maximum effect of alamethicin was found to be almost 3 times as high as that of **1**.

Even though it was not as potent as the reference peptide, it is clear that **1** causes leakage through simplistic lipid membrane models in the form of liposomes as well as from whole cells. However, the results do not reveal the exact mode of that leakage, that is, if the protein forms small well-defined pores or larger fissures, or breaks in the membrane, or breaks it up through a detergent-like effect. Compared to the results for alamethicin, a well-characterized pore-forming peptide,[28] both the slope of the concentration−response curves and the maximum effect differed significantly for **1** in the liposome assay. This indicates that these two compounds do not affect the membrane in the same manner, and hence **1** does not form small distinct pores, as does alamethicin. On the other end of the spectrum is a detergent-like effect, in which **1** would simply dissolve the lipid membranes. If that were the case, all liposome content should be released, and hence the maximum effect of **1** should be at least the same as for alamethicin. However the maximum effect of **1** was only approximately a third of that for alamethicin, which makes a complete dissolution of the membrane highly unlikely. Taken together, our results suggest that **1** acts through a pore-forming mechanism different from that of alamethicin.

In our previous work regarding the cytotoxic activities of the cyclotides, we pointed out both structural and functional similarities between the cyclotides and the defensin family of antimicrobial peptides.[23,24] For example, defensins have anticancer effects in the same concentration interval as cyclotides, and they show similar, very sharp profiles in their dose−response curves (i.e., an "on−off" effect).[29,30] Furthermore, and by analogy with the results in the present study, defensins have been shown to permeabilize lipid membranes in a not yet fully defined mechanism.[31−33] However, defensins also act through intracellular as well as nonmembrane external targets.[34,35] Whether or not this is also the case for the cyclotides remains to be shown.

Membrane-disruptive properties of cyclotides may also explain many of the other activities that have been reported for this protein family: their antimicrobial, hemolytic, and insecticidal effects are likely all connected to membrane disruption. In addition, the same mechanism may explain the seemingly more specific effects that have been reported for some cyclotides. For example, the uterotonic activity of kalata B1[11] and the neurotensin antagonist activity of cyclopsychotride A[36] appear to be results of specific mechanisms, such as a single receptor−ligand interaction. However, if kalata B1 disrupts cell membranes, Ca^{2+} will be one of the ions to move across the membrane, thus mediating muscle contraction—in this case, of the uterus. Cyclopsychotride A was indeed shown to increase intracellular Ca^{2+} levels in a concentration-dependent manner,[36] which could not be blocked by a known neurotensin antagonist. In addition, this cyclotide showed a similar behavior in two unrelated cell lines that did not express neurotensin receptors, which suggested that it acts through another mechanism.[36] In light of the results in the present study, the mechanism of action of cyclopsychotride A is conceivably membrane disruption.

Membrane-active peptides are considered a promising lead toward new anticancer agents that offer an improvement and

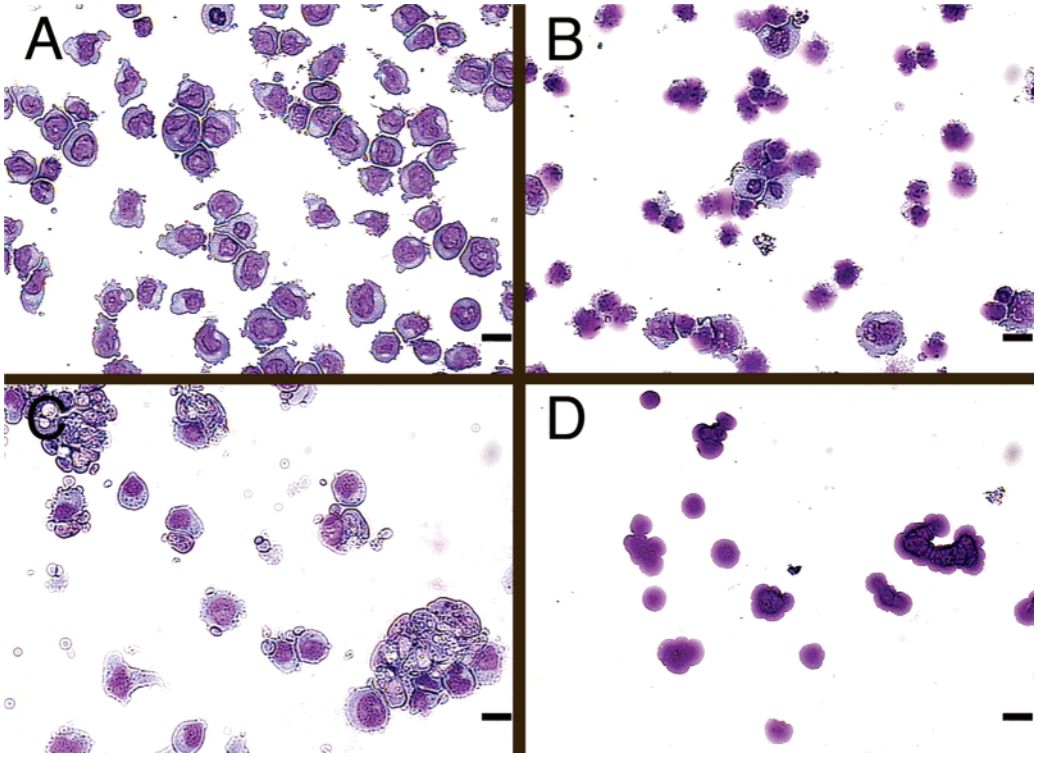

Figure 3. Gross morphology after 4 h. Panel A shows viable cells in the control. Cells exposed to 4 μM cycloviolacin O2 (**1**) (B) and 1% Triton X-100 (D) display predominantly disintegrated membranes, while cells exposed to 25 μM etoposide (C) display condensed, fragmented nuclei and intact membranes. The bar equals 20 μm.

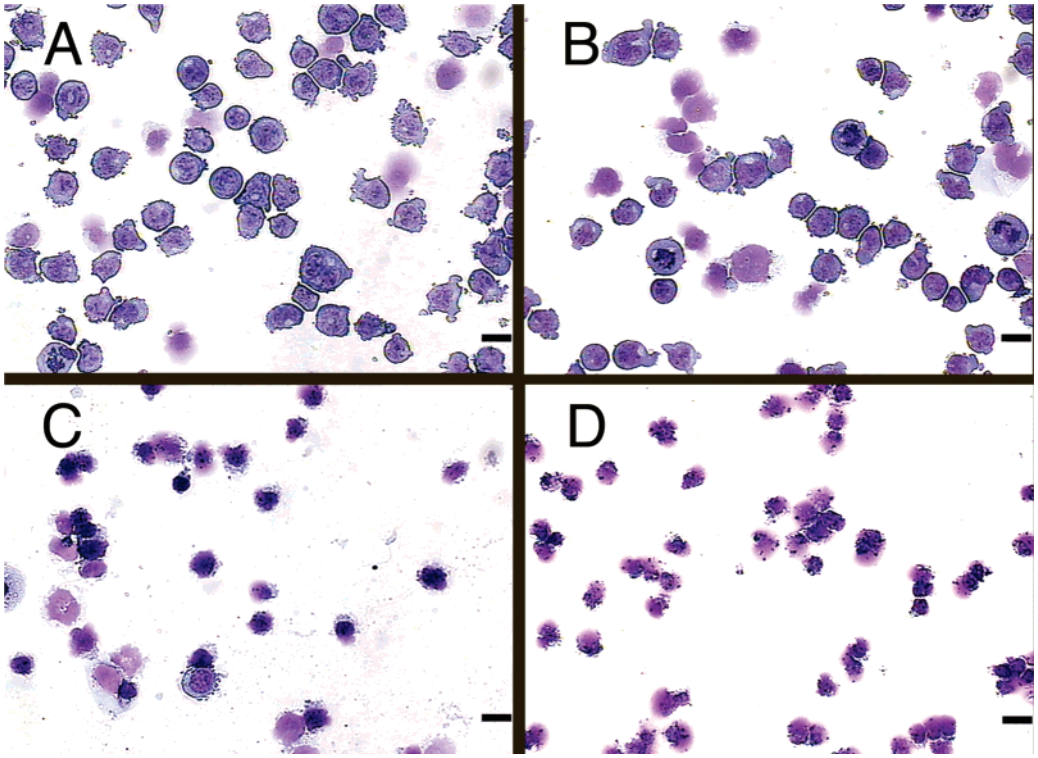

Figure 4. Cycloviolacin O2 (**1**)-induced changes in gross morphology over time. Prolonged exposure to **1** (4 μM) increases the number of cells with disrupted cell membranes, as shown by the microphotographs taken after 5 min (A), 15 min (B), 60 min (C), and 24 h (D). The bar equals 20 μm.

adjuvant to currently used cancer chemotherapeutic drugs.[37,38] For example, they interact with the cancer cells within minutes, their broad spectrum cytotoxic activity is independent of known drug resistance mechanisms, and they show slightly selective effects against cancer cells compared to normal cells. For clinical use, however, these peptides also need a high stability.[38] In this context cyclotides provide a unique opportunity; the CCK motif is an extremely stable scaffold[4,5] that can host a diverse set of sequences in its surface exposed loops. In addition, cyclotides display a definite structure−activity relationship,[23,24] which can be modulated to change the cytotoxic activity.[25] Together with the wealth of native cyclotides that await discovery and testing,[6] and since cyclotides

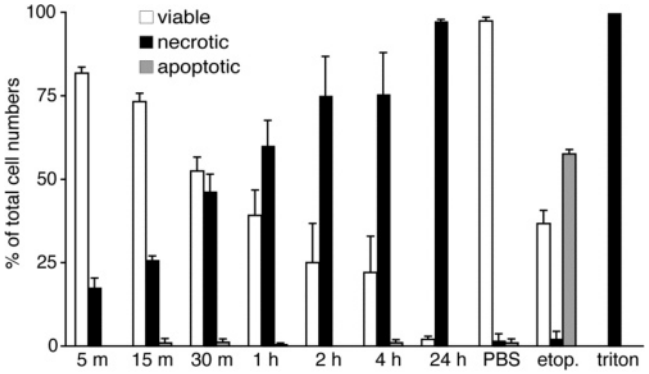

Figure 5. Summary of cell counts from 5 min to 24 h. Dead cells were classified according to their gross morphology as necrotic (i.e., cells that display predominantly disintegrated membranes) or apoptotic (i.e., cells that display condensed, fragmented nuclei and intact membranes). For comparison counts for the control (PBS), 25 μM etoposide (etop.), and 1% Triton X-100 (triton) are shown. The bars represent mean values ± SEM.

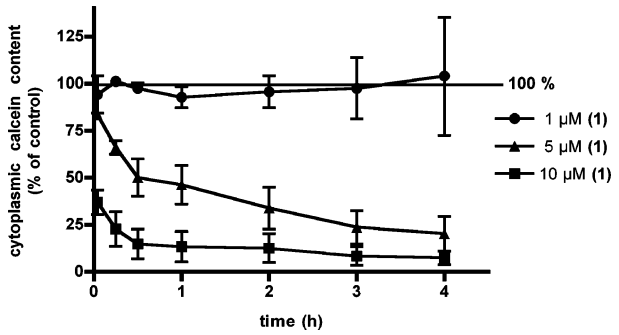

Figure 6. Membrane effects on HeLa cells. Cells loaded with calcein were exposed to three different concentrations of cycloviolacin O2 (**1**). The effect and the kinetics of the effect are concentration dependent. Each point represents the mean, while the error bars indicate ± SEM.

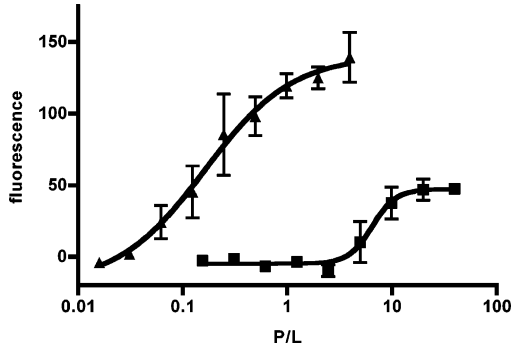

Figure 7. Membrane effects on POPC liposomes. Concentration−response curve of alamethicin (triangles) and cycloviolacin O2 (**1**) (squares) in the Tb^{3+}/DPA-based liposome assay.

can now be produced through chemical synthesis[8] and by expression of intein fusion proteins in *E. coli*,[39] this provides the basis for a rational approach to explore the cytotoxic effects of the cyclotides.

In conclusion, this is the first report on the cytotoxic mechanism of action of the cyclotides. The results show clearly that a rapid membrane disruption plays a crucial role for the cytotoxic effect of **1**. In addition, membrane interactions provide a plausible explanation for the diverse set of activities displayed by other members of this unique protein family.

Experimental Section

General Experimental Procedures. Glutamine, penicillin, streptomycin, fluorescein diacetate, PBS, and heat-inactivated fetal calf serum (FCS) were obtained from Sigma (St. Louis, MO). Water was of Millipore grade. Cell-growth medium RPMI 1640 (HyClone, Logan, UT) was supplemented with 10% FCS, 2 mM glutamine, 50 μg/mL streptomycin, and 60 μg/mL penicillin. Stock solution of etoposide (Vepeside) was obtained from Bristol-Myers Squibb, Triton X-100 was obtained from Acros Organics (Geel, Belgium), and alamethicin was obtained from ICN Biomedicals Inc. (Aurora, OH). Cycloviolacin O2 (**1**), cyclo-(GIPCGESCVWIPCISSAIGCSCKSKVCYRN), was isolated from aerial and dried parts of *Viola odorata* L. (Violaceae) (obtained from Galke, Gittelde, Germany), as described previously.[7,40] Purity of the isolated cyclotide was >95% as determined by RP-HPLC. The human lymphoma cell line U-937 GTB was used for the FMCA and the microscopy studies, and HeLa cells were used for the calcein assay. This cell line is considered to be sensitive to a wide range of cytotoxic agents and has not exhibited any known drug resistance. The cell line was procured and maintained as described earlier.[41,42]

Fluorometric Microculture Cytotoxicity Assay (FMCA). Cytotoxicity was measured using the FMCA as reported previously.[41,42] For the assay, **1** was dissolved in water of Millipore grade to a concentration of 40 μM. Dilution series were made at a 1:1 ratio from the stock solution. Then, V-shaped, 96-well microtiter plates (Nunc A/S, Roskilde, Denmark) were prepared using 20 μL per well of cyclotide test solution in duplicates for each concentration. In addition, six blank wells (200 μL per well of cell-growth medium) and six negative-control wells (20 μL per well of PBS) were prepared on each microtiter plate.

Initial cell viability was assessed using the trypan blue dye exclusion test. Cancer cells suspended in cell-growth medium were dispensed on the prepared microtiter plates (20 000 cells/180 μL per well previously filled with 20 μL of test solution at 10 times the desired concentration) and incubated for 4, 8, 24, and 72 h at 37 °C and 5% CO_2. After incubation the cells were washed with PBS, and 100 μL of fluorescein diacetate (10 μg/mL) was added to each well. The plates were incubated at 37 °C and 5% CO_2 for 40 min, and fluorescence was then measured in a 96-well scanning spectrofluorometer at 538 nm, following excitation at 485 nm.[42] Survival index (SI) and IC_{50} values were calculated and validated as described previously.[41] All experiments were repeated twice.

Microscopy Studies. V-shaped, 96-well microtiter plates (Nunc A/S, Roskilde, Denmark) were prepared with 20 μL of sample per well; PBS was used as a control, and **1** (40 μM), etoposide (250 μM), and Triton X-100 (10%) were dissolved in water of Millipore grade. Tumor cells suspended in cell-growth medium were then dispensed on the prepared microtiter plates (20 000 cells in 180 μL of medium per well previously filled with 20 μL of test solution at 10 times the desired concentration) and incubated at 37 °C and 5% CO_2. Microscope slides from each well were prepared using a Shandon Cytospin 3 centrifuge (Thermo Fischer Scientific Inc., Waltham, MA) after 5 min, 15 min, 30 min, 1 h, 2 h, 4 h, and 24 h for cells exposed to 4 μM **1**. For control cells and cells exposed to 1% Triton X-100 or 25 μM etoposide, slides were prepared after 4 h.

Slides were stained according to the May-Grünwald-Giemsa (MGG) method and then air-dried. A quantitative measure of the gross morphology was obtained by classifying the cells as necrotic or apoptotic. Cells with disintegrated membranes were classified as necrotic, and cells with a condensed, fragmented nucleus and intact membranes were classified as apoptotic. Cells in a late stage of apoptosis, that is, having a condensed fragmented nucleus and disintegrated membranes, were also classified as apoptotic. About 200 cells per slide were examined in three different randomized areas on each slide.

Calcein Assay. Cancer cells were incubated in 96-well microtiter plates with a flat bottom (Nunc A/S, Roskilde, Denmark). Calcein acetoxymethyl ester (Molecular Probes, Eugene, OR) was added to the incubated cells. Then, **1** was added at concentrations from 1 to 10 μM, and PBS was used as a control. The fluorescence of the entrapped calcein in each cell was measured with an ArrayScan (Cellomics Inc., Pittsburgh, PA) after 5 min, 15 min, 30 min, 1 h, 2 h, 3 h, and 4 h. The experiment was repeated twice.

Tb^{3+}/DPA Liposome Assay. The Tb^{3+}/DPA liposome assay as described by Rausch and Wimley[27] was modified so as to give a quantitative format. Chloroform stock solutions of the lipid 1-palmitoyl-2-oleoyl-*sn*-glycero-3-phosphocholine (POPC; Avanti Polar Lipids Inc., Alabaster, AL) were dried in round-bottomed flasks *in vacuo* for 3 h to form a thin film. The film was further dried overnight *in vacuo* in

a desiccator and then hydrated with buffer 1 (50 mM $TbCl_3$, 85 mM Na_3 citrate, 10 mM TES, pH 7) by extensive vortexing to form a 100 mM lipid suspension. The suspension was subjected to 10 freeze−thaw cycles to ensure the formation of unilamellar liposomes and maximum entrapment of Tb^{3+}. The liposomes were extruded 25 times through a 100 nm polycarbonate filter mounted in a Mini-Extruder (Avanti Polar Lipids Inc., Alabaster, AL). External Tb^{3+} was removed by means of gel filtration on a Sephadex G-25 column (Amersham Biosciences, Uppsala, Sweden) eluted with buffer 2 (290 mM NaCl, 10 mM TES, pH 7), and the POPC concentration was determined using the Stewart assay.[43]

For the liposome assay, **1** was dissolved in buffer 2 to a concentration of 200 μM and the positive control alamethicin dissolved in buffer 2 to a concentration of 20 μM. Dilution series were made at a 1:1 ratio from the stock solutions. The assay was carried out in V-shaped, 96-well microtiter plates (Nunc A/S, Roskilde, Denmark). Test solutions (50 μL per well) were incubated for 1 h with POPC liposomes (total lipid concentration 2.2 μM) and 3 μM external DPA at room temperature. The total volume in the wells during incubation was 115 μL.

Fluorescence was measured manually at room temperature by taking 100 μL from each well and adding this to 400 μL of buffer 2 in the spectrofluorometer. The excitation/emission wavelengths used were 260/545 nm. All experiments were repeated three times. EC_{50} values were calculated using nonlinear regression and the sigmoidal dose−response (variable slope) equation in GraphPad Prism4 (GraphPad Software, San Diego, CA).

Acknowledgment. We thank Prof. M. Lang, Division of Pharmaceutical Biochemistry, Department of Pharmaceutical Biosciences, Uppsala University, and M. Wickström, Division of Clinical Pharmacology, Department of Medical Sciences, Uppsala University, for technical advice.

References and Notes

(1) Craik, D. J.; Daly, N. L.; Bond, T.; Waine, C. *J. Mol. Biol.* **1999**, *294*, 1327−1336.
(2) Göransson, U.; Craik, D. J. *J. Biol. Chem.* **2003**, *278*, 48188−48196.
(3) Rosengren, K. J.; Daly, N. L.; Plan, M. R.; Waine, C.; Craik, D. J. *J. Biol. Chem.* **2003**, *278*, 8606−8616.
(4) Gran, L. *Lloydia* **1973**, *36*, 174−178.
(5) Colgrave, M. L.; Craik, D. J. *Biochemistry* **2004**, *43*, 5965−5975.
(6) Simonsen, S. M.; Sando, L.; Ireland, D. C.; Colgrave, M. L.; Bharathi, R.; Göransson, U.; Craik, D. J. *Plant Cell* **2005**, *17*, 3176−3189.
(7) Göransson, U.; Svangård, E.; Claeson, P.; Bohlin, L. *Curr. Protein Pept. Sci.* **2004**, *5*, 317−329.
(8) Craik, D. J.; Daly, N. L.; Mulvenna, J.; Plan, M. R.; Trabi, M. *Curr. Protein Pept. Sci.* **2004**, *5*, 297−315.
(9) Ireland, D. C.; Colgrave, M. L.; Craik, D. J. *Biochem. J.* **2006**, *400*, 1−12.
(10) Mulvenna, J. P.; Wang, C.; Craik, D. J. *Nucleic Acids Res.* **2006**, *34*, D192−194.
(11) Gran, L. *Acta Pharmacol. Toxicol.* **1973**, *33*, 400−408.
(12) Schöpke, T.; Hasan, Agha, M. I.; Kraft, R.; Otto, A.; Hiller, K. *Sci. Pharm.* **1993**, *61*, 145−153.
(13) Simonsen, S. M.; Daly, N. L.; Craik, D. J. *FEBS Lett.* **2004**, *577*, 399−402.
(14) Tam, J. P.; Lu, Y. A.; Yang, J. L.; Chiu, K. W. *Proc. Natl. Acad. Sci. U.S.A.* **1999**, *96*, 8913−8918.
(15) Gustafson, K. R.; McKee, T. C.; Bokesch, H. R. *Curr. Protein Pept. Sci.* **2004**, *5*, 331−340.
(16) Göransson, U.; Sjögren, M.; Svangård, E.; Claeson, P.; Bohlin, L. *J. Nat. Prod.* **2004**, *67*, 1287−1290.
(17) Jennings, C.; West, J.; Waine, C.; Craik, D.; Anderson, M. *Proc. Natl. Acad. Sci. U.S.A.* **2001**, *98*, 10614−10619.
(18) Craik, D. J. *Science* **2006**, *311*, 1563−1564.
(19) Craik, D. J.; Cemazar, M.; Daly, N. L. *Curr. Opin. Drug Discovery Dev.* **2006**, *9*, 251−260.
(20) Daly, N. L.; Gustafson, K. R.; Craik, D. J. *FEBS Lett.* **2004**, *574*, 69−72.
(21) Kamimori, H.; Hall, K.; Craik, D. J.; Aguilar, M. I. *Anal. Biochem.* **2005**, *337*, 149−153.
(22) Shenkarev, Z. O.; Nadezhdin, K. D.; Sobol, V. A.; Sobol, A. G.; Skjeldal, L.; Arseniev, A. S. *FEBS J.* **2006**, *273*, 2658−2672.
(23) Lindholm, P.; Göransson, U.; Johansson, S.; Claeson, P.; Gullbo, J.; Larsson, R.; Bohlin, L.; Backlund, A. *Mol. Cancer Ther.* **2002**, *1*, 365−369.
(24) Svangård, E.; Göransson, U.; Hocaoglu, Z.; Gullbo, J.; Larsson, R.; Claeson, P.; Bohlin, L. *J. Nat. Prod.* **2004**, *67*, 144−147.
(25) Herrmann, A.; Svangård, E.; Claeson, P.; Gullbo, J.; Bohlin, L.; Göransson, U. *Cell. Mol. Life Sci.* **2006**, *63*, 235−245.
(26) Neri, S.; Mariani, E.; Meneghetti, A.; Cattini, L.; Facchini, A. *Clin. Diagn. Lab. Immunol.* **2001**, *8*, 1131−1135.
(27) Rausch, J. M.; Wimley, W. C. *Anal. Biochem.* **2001**, *293*, 258−263.
(28) Duclohier, H. *Eur. Biophys. J.* **2004**, *33*, 169−174.
(29) Barker, E.; Reisfeld, R. A. *Cancer Res.* **1993**, *53*, 362−367.
(30) Bateman, A.; Singh, A.; Jothy, S.; Fraser, R.; Esch, F.; Solomon, S. *Peptides* **1992**, *13*, 133−139.
(31) Fujii, G.; Selsted, M. E.; Eisenberg, D. *Protein Sci.* **1993**, *2*, 1301−1312.
(32) Kagan, B. L.; Selsted, M. E.; Ganz, T.; Lehrer, R. I. *Proc. Natl. Acad. Sci. U.S.A.* **1990**, *87*, 210−214.
(33) Zasloff, M. *Nature* **2002**, *415*, 389−395.
(34) Lehrer, R. I. *Nat. Rev. Microbiol.* **2004**, *2*, 727−738.
(35) Brogden, K. A. *Nat. Rev. Microbiol.* **2005**, *3*, 238−250.
(36) Witherup, K. M.; Bogusky, M. J.; Anderson, P. S.; Ramjit, H.; Ransom, R. W.; Wood, T.; Sardana, M. *J. Nat. Prod.* **1994**, *57*, 1619−1625.
(37) Leuschner, C.; Hansel, W. *Curr. Pharm. Des.* **2004**, *10*, 2299−2310.
(38) Papo, N.; Shai, Y. *Cell. Mol. Life Sci.* **2005**, *62*, 784−790.
(39) Kimura, R. H.; Tran, A. T.; Camarero, J. A. *Angew. Chem., Int. Ed.* **2006**, *45*, 973−976.
(40) Claeson, P.; Göransson, U.; Johansson, S.; Luijendijk, T.; Bohlin, L. *J. Nat. Prod.* **1998**, *61*, 77−81.
(41) Dhar, S.; Nygren, P.; Csoka, K.; Botling, J.; Nilsson, K.; Larsson, R. *Br. J. Cancer* **1996**, *74*, 888−896.
(42) Larsson, R.; Nygren, P. *Anticancer Res.* **1989**, *9*, 1111−1119.
(43) Stewart, J. C. *Anal. Biochem.* **1980**, *104*, 10−14.

NP070007V